3-S1-15

Simulating the sound generation in flutes and flue pipes with the Lattice-Boltzmann-Method

Helmut Kühnelt[1]

[1]Institute of Musical Acoustics (IWK),
University of Music and Performing Arts Vienna, Austria
kuehnelt@mdw.ac.at

Abstract

In flue instruments like flutes, recorders or labial organ pipes, the non-linear interaction between jet flow and sound field is the driving source for sound generation. In a mesoscopic approach, the Lattice-Boltzmann-Method (LBM) simulates the time-dependent motion of an ideal gas governed by the compressible Navier-Stokes equations in the low Mach number regime including acoustics and fluid dynamics intrinsically. Therefore LBM is a reasonable candidate for simulating flow-acoustic interaction.

This paper reports ongoing research and gives more detailed results of three-dimensional simulations of the sound generation in flue pipes. The behavior of the oscillating system is analyzed in the time and frequency domain and the generated acoustical power is studied.

1. The Lattice Boltzmann Method

A fluid is commonly viewed as a macroscopic continuum with properties varying in space and time. The temporal and spatial evolution of density, velocity and energy are described by the nonlinear Navier-Stokes equations which are in general difficult to solve.

Taking a different, a mesoscopic view at the fluid, the question of how many fluid molecules having a velocity vector in the vicinity of $\vec{\xi}$ are found in an infinitesimal small volume element around $\vec{r}$ at a certain time t can be answered statistically by introducing a particle distribution function $f(\vec{r}, \vec{\xi}, t)$. The macroscopic quantities density ρ, momentum density $\rho\vec{u}$ and internal energy density $\rho\epsilon$ are then obtained by evaluating the moments of the distribution function:

$$\begin{bmatrix} \rho(\vec{r},t) \\ \rho(\vec{r},t)\vec{u}(\vec{r},t) \\ \rho(\vec{r},t)\epsilon(\vec{r},t) \end{bmatrix} = \int \begin{bmatrix} 1 \\ \vec{\xi} \\ \frac{(\vec{\xi}-\vec{u})^2}{2} \end{bmatrix} f(\vec{r},\vec{\xi},t) d\vec{\xi} \quad (1)$$

As we will only consider isothermal systems, we skip ϵ.

The equation of motion for the distribution function is the Boltzmann equation:

$$\left(\frac{\partial}{\partial t} + \nabla_r \cdot \vec{\xi}\right) f(\vec{r},\vec{\xi},t) = \Omega \quad (2)$$

It states that only collisions Ω change the otherwise constant flow of particles. If the fluid evolves without external forcing it will approach equilibrium given by the Maxwell-Boltzmann distribution:

$$f^{(eq)}(\vec{\xi}) = \frac{\rho}{(2\pi RT)^{3/2}} e^{-\frac{(\vec{\xi}-\vec{u})^2}{2RT}} \quad (3)$$

The moments of the Boltzmann equation are the hydrodynamic equations. If the motion of the fluid is determined only by fast convection and slow diffusion, the Navier-Stokes equations can be recovered in the macroscopical limit. As the Boltzmann equation is more general than the Navier-Stokes equations, it describes a greater class of systems.

Two major difficulties practically arise in solving the Boltzmann equation. First there are enormous degrees of freedom as the velocity ranges from $-\infty$ to $+\infty$, and second the collision operator includes in general nonlinearities. Systems we are interested in, like the dynamics of the jet in a flute are in the low Mach number regime. So the task is to find the most simple low Mach number approximation of the Boltzmann equation that is able to reproduce the correct macroscopic dynamics and to overcome the above mentioned difficulties. Here the main steps to the Lattice Boltzmann Method (LBM) will be described in short, for further information see [1] and references within.

Discretization in space and time leads to a discrete Boltzmann equation still continuous in the velocity:

$$f(\vec{r}+\vec{\xi}\delta_t, t+\delta_t) - f(\vec{r},t) = -1/\tau\left(f - f^{(eq)}\right) \quad (4)$$

This introduces a spatial and temporal lattice. Here we also introduced the BGK model of the collision operator assuming that the system relaxes linearly to equilibrium with constant rate $1/\tau$.

Discretization of the velocity space is a crucial step: To preserve the conservation laws exactly, the hydrodynamic moments (ρ, $\rho\vec{u}$) must be evaluated exactly:

$$\rho = \int f^{(eq)} d\vec{\xi} = \sum_\alpha f_\alpha^{(eq)} = \sum_\alpha f_\alpha, \quad (5)$$

$$\rho\vec{u} = \int \vec{\xi} f^{(eq)} d\vec{\xi} = \sum_\alpha \vec{c}_\alpha f_\alpha^{(eq)} = \sum_\alpha \vec{c}_\alpha f_\alpha \quad (6)$$

This procedure that determines the set of possible velocities $\vec{c}_\alpha$ has to be applied up to the fourth-order moments to ensure the isotropy of the macroscopic quantities and the stress tensor. This leads to minimal sets of 6 or 9 velocity vectors in two dimensions and of 15 or 19 velocities in three dimensions.

As the continuous equilibrium distribution can't be summed up as above, it has to be approximated for low Mach numbers

$$f_\alpha^{(eq)} = w_\alpha \rho \left(1 + \frac{\vec{c}_\alpha \cdot \vec{u}}{c_s^2} + \frac{(\vec{c}_\alpha \cdot \vec{u})^2}{2c_s^4} - \frac{\vec{u}^2}{2c_s^2}\right) \quad (7)$$

with weights w_α depending on the chosen lattice.

If the lattice spacing δ_t is set so that in one timestep δ_t the f_α are transported to the neighboring lattice nodes ($\delta_t/\delta_t = 1$), the lattice Boltzmann equation (LBE) reads:

$$\begin{aligned} f_\alpha(\vec{r} + \vec{c}_\alpha, t+1) = \\ f_\alpha(\vec{r}, t) - 1/\tau \left(f_\alpha(\vec{r}, t) - f_\alpha^{(eq)}(\vec{r}, t)\right) \end{aligned} \quad (8)$$

This simple and efficient computable update-rule can be split up in a local collision step and a propagation only involving communication with neighbor grid points. In the macroscopic limit ($\delta_x, \delta_t \to 0$) the LBE recovers the Navier-Stokes equations with the equation of state of an ideal isothermal gas ($p = c_s^2\rho$) and a viscosity depending on the relaxation time ($\nu = c_s^2(\tau - 1/2)$) with sound speed $c_s = 1/\sqrt{3}$.

To enhance the stability in the low viscosity regime a multi-relaxation-time LBM was introduced by Lallemand [2] and extended to three dimension by d'Humières [3]. It optimizes the transport coefficients (sound speed, viscosity, etc.) by adjusting free parameters and greatly enhances stability by decoupling physical and non-physical (lattice) modes via different relaxation times. This algorithm was used for the presented simulations.

Local boundary conditions can easily constructed such as bounce-back for rigid walls, where all incident distributions are reflected exactly 180 degrees leading to zero velocity at the wall. Acoustical systems are very sensitive to the treatment of acoustic waves at boundaries. Therefore non-reflecting boundary conditions were implemented using extrapolation of the velocity and a linear relaxation method [4] for the density combined with an interior zone where the shear stresses are smoothed out by gradually increasing the relaxation times to 1. Due to a suboptimal choice of the relaxation parameter there remains a small degree of reflection at the boundary which can be observed in the simulations.

2. Three-dimensional flute simulation with LBM

2.1. Geometry and simulation parameters

A small stopped pipe was simulated. The resonator measures 60 × 10 × 10 mm, the flue 15 × 7 × 1.5 mm. The ratio of the distance from the flue exit to the labium to the height of the flue exit is 7 mm / 1.5 mm = 4.67, which is close to the value of about 4 often observed in recorders. The angle of the labium is $14°$. The surrounding volume above the pipe is 75 mm × 10 mm × 38 mm. The lattice resolution was chosen rather large, $\delta_x = 0.3$ mm. The timestep which is connected to the lattice spacing via the relation $\delta_x/\delta_t = c_{sound}^{real}/c_{sound}^{LBM}$ is approx. $5 \cdot 10^{-7}$ s.

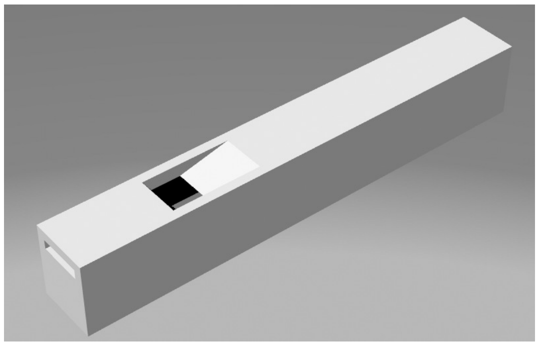

Figure 1: Simulated stopped pipe.

To smooth out parasitic short-wavelength fluctuations due to large gradients at sharp edges, the kinematic viscosity was set to $3 \cdot 10^{-4} \mathrm{m}^2/\mathrm{s}$, 20 times larger that the viscosity of air and the bulk viscosity was also set to a rather high value of $2 \cdot 10^{-3} \mathrm{m}^2/\mathrm{s}$. Therefore higher viscous losses for both, the fluid motion and the acoustic field have to be expected. That's why a higher jet speed is needed to reach the oscillating regime.

2.2. Time and frequency domain behavior

Fig. 2 shows the oscillating density, which is related to the sound pressure via the equation of state at the stopped end of the pipe during the startup and as the steady-state is reached. After a rather short rising time of 2500 timesteps (1.27 ms) the velocity of the flow in the flue reaches a maximum value of 0.062 (36.5 m/s) and approaches a stable value of 0.057 (33.6 m/s) after 5000 timesteps (2.54 ms). The flute works in its first mode. In the spectrum taken outside at the middle, 26 mm above the flute (Fig. 3) the third (-46 dB) and the fifth harmonic (-57 dB) (arrows) are present but not very pronounced. In other simulations the pipe was overblown to the twelfth with a sounding frequency about 65 cent lower than the expected harmonic. This indicates a non-harmonic relation of the pipe resonances as expected in pipes with non-flaring cross section. That is why the present spectrum is harmonically so poor. Even harmonics that are

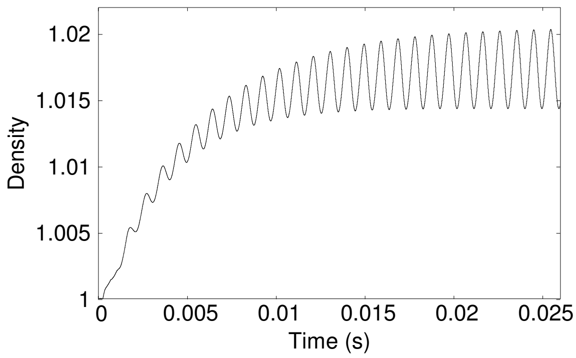

(a)

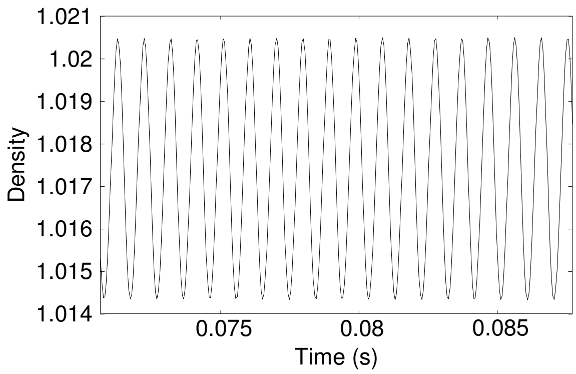

(b)

Figure 2: Density at the stopped end of the pipe during (a) startup and (b) steady-state oscillations.

also seen are artifacts due to acoustic reflections from the outflow boundaries as mentioned above. Nevertheless the contribution of these distortions is less than 3% of the amplitude of the fundamental.

During steady state operation a sound pressure level of 140 dB is reached at the stopped end of the pipe, outside the flute at a distance of 26 mm above the flute a sound pressure level of 121 dB is measured.

2.3. Motion of the jet around the labium

Fig. 4 shows the iso-velocity surface at $v = 0.017$ (10 m/s). Near to the lateral boundary the jet velocity is steady in an upward direction. Only the middle part of the jet swings around the labium and enters the flute. This affects the sound production as will be shown below.

2.4. Flow sound interaction in the mouth of the instrument – Production of acoustical energy

The interaction of the vortical jet flow with the sound field converts either rotation into acoustical energy or the other way round acoustical energy into rotation, thus producing or absorbing sound. According to Howe [5] the principal contribution of sound for a compact source re-

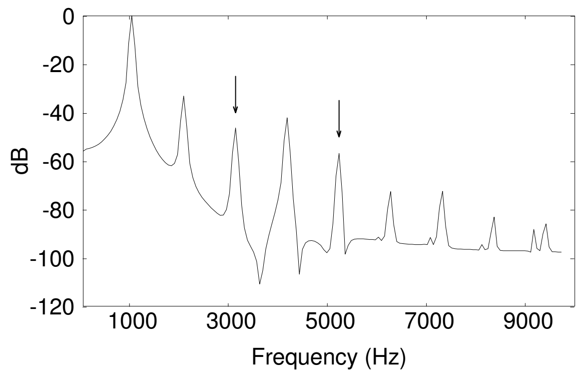

Figure 3: Steady-state sound-spectrum (a) outside and (b) inside the flute at the stopped end.

gion (small compared to the acoustical wavelength) at low Mach numbers is caused by the source density

$$\vec{f} = -\rho_0(\vec{\omega} \times \vec{v}). \tag{9}$$

At this level of approximation the acoustic power generated is the integral

$$P_{ac} = -\int_V \overline{\rho_0(\vec{\omega} \times \vec{u}) \cdot \vec{u}'} dV \tag{10}$$

over the source volume V of the time average of the triple product between the vorticity $\vec{\omega}$, the acoustic velocity $\vec{u}'$ and the flow velocity $\vec{u}$ [6]. The acoustical velocity $\vec{u}'$ is the unsteady irrotational component of the total velocity field $\vec{v}$ and the flow velocity $\vec{u}$ excludes the acoustical velocity.

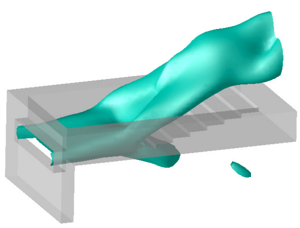

(a) $t = 0T_0$

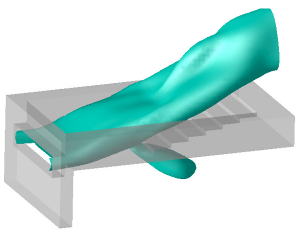

(b) $t = 5/19T_0$

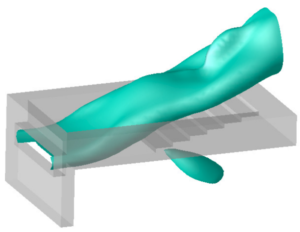

(c) $t = 10/19T_0$

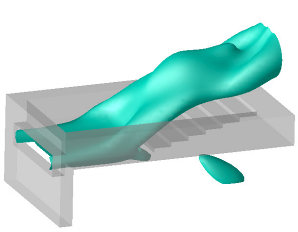

(d) $t = 15/19T_0$

Figure 4: Motion of the jet around the labium during one period T_0. Iso-velocity surface at $v = 0.017$.

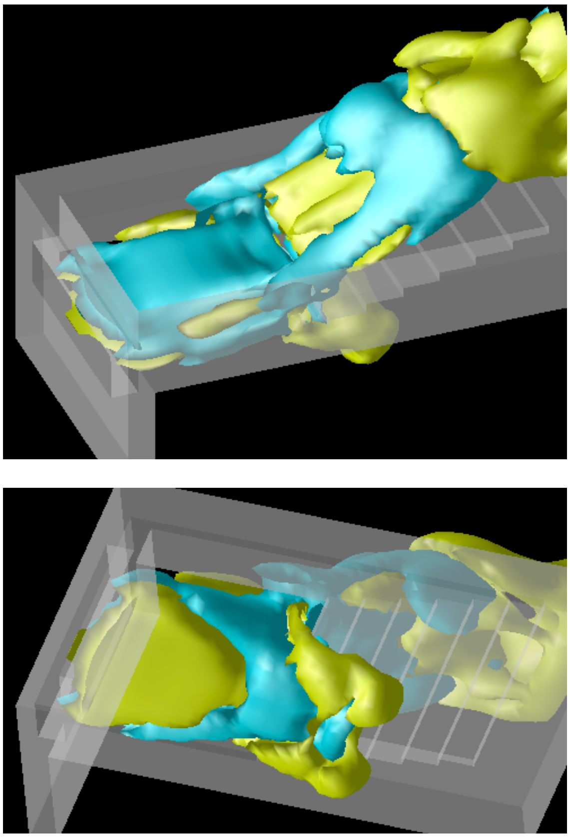

Figure 5: Surfaces of equal power at $\pm 7.5 \cdot 10^{-8}$ of the sound produced (yellow) and absorbed (blue) by flow acoustic interaction as the acoustic velocity in the mouth of the flute has reached its maximum value and points outwards the flute (top and bottom view).

The upper and the lower shear layer of the jet can both act as sound sources or sinks depending on the angle between $\vec{\omega} \times \vec{u}$ and $\vec{u}'$. To get an impression of the complicated three-dimensional source distribution in the mouth of the flute, Fig. 5 shows surfaces of equal power of produced and absorbed sound. An integration in the direction transverse to the jet (y-direction) averaged over the hole period (Fig. 6) shows areas acting as sources (yellow to red) and as sinks (blue). There are two main source areas, a weaker one downstream the flue exit and a strong one near the edge of labium which continues downstream and covers the region above the labium. The sound sink in the middle of the mouth is less strong than the source, so that there is a overall surplus of acoustical power of approximately 0.23 mW/s if converted into realistic unities.

3. Conclusions

Simulating the three-dimensional flow acoustic process of self-sustained oscillations in a flute, the lattice Boltzmann method demonstrated its ability to solve coupled flow-acoustic problems in realistic geometries. Up to now the results of the simulations are difficult to compare with reality because of the quite high viscosity chosen, but the results are reasonable. On the way to quantitative simulations some technical problems have to be solved, especially to be able to simulate larger volumina with better resolution at realistic viscosities. Then the comparison with experiments will help to open the way towards a flute- and head-joint-simulator which can be used to determine parameters important for musicians or instrument makers as sound quality, sound level, efficiency, attack or response.

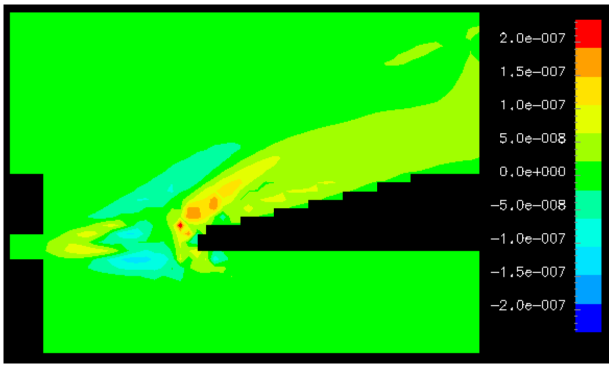

Figure 6: Acoustic source power averaged over one period.

References

[1] Succi, S., The Lattice Boltzmann Equation for Fluid Dynamics and Beyond, Oxford University Press, Oxford, 2001.

[2] Lallemand, P. and Luo, L.S., “Theory of the Lattice Boltzmann Method: Dispersion, Dissipation, Isotropy, Galilean Invariance, and Stability”, Physical Review E, 61(6):6546–62, 2000.

[3] d’Humières, D., Ginzburg, I., Krafczyk, M., Lallemand, P. and Luo, L.S., “Multiple-relaxation-time lattice Boltzmann models in three dimensions”, Phil. Trans. R. Soc. Lond. A, 360:437–51, 2002.

[4] Poinsot,T. and Lele, S., “Boundary conditions for direct simulations of compressible viscous flows”, J. Comput. Phys., 101(1):104–129,1992.

[5] Howe, M.S., The Theory of Vortex Sound, Cambridge University Press, Cambridge, 2003

[6] Jenvey, P.L., “The sound power from turbulence: A theory of the exchange of energy between the acoustic and non-acoustic fields”, J. Sound Vib.,131(1):37–66,1989.